

PAPER • OPEN ACCESS

Influence of Ar gas pressure on ion energy and charge state distributions in pulsed cathodic arc plasmas from Nb–Al cathodes studied with high time resolution

To cite this article: Siegfried Zöhrer *et al* 2019 *J. Phys. D: Appl. Phys.* **52** 055201

View the [article online](#) for updates and enhancements.

You may also like

- [Josephson junctions and DC SQUIDS based on Nb/Al technology](#)
J Flokstra, D J Adelerhof, E P Houwman *et al.*
- [Universality of transport properties of ultrathin oxide films](#)
V Lacquaniti, M Belogolovskii, C Cassiago *et al.*
- [Time-resolved ion energy and charge state distributions in pulsed cathodic arc plasmas of NbAl cathodes in high vacuum](#)
Siegfried Zöhrer, André Anders and Robert Franz

Recent citations

- [Erosion and cathodic arc plasma of Nb–Al cathodes: composite versus intermetallic](#)
Siegfried Zöhrer *et al*
- [Influence of shielding gas on cathode spot behaviours in alternating current tungsten inert gas welding of aluminium](#)
Le Huy Phan *et al*
- [Experimental Chemistry and Structural Stability of AlNb₃ Enabled by Antisite Defects Formation](#)
Nikola Koutná *et al*



The Electrochemical Society
Advancing solid state & electrochemical science & technology

241st ECS Meeting

May 29 – June 2, 2022 Vancouver • BC • Canada

Abstract submission deadline: Dec 3, 2021

Connect. Engage. Champion. Empower. Accelerate.
We move science forward



Submit your abstract



Influence of Ar gas pressure on ion energy and charge state distributions in pulsed cathodic arc plasmas from Nb–Al cathodes studied with high time resolution

Siegfried Zöhrer^{1,4} , André Anders^{2,3}  and Robert Franz¹ 

¹ Montanuniversität Leoben, Leoben, Austria

² Lawrence Berkeley National Laboratory, Berkeley, CA, United States of America

E-mail: szoehrer@alumni.tugraz.at

Received 30 August 2018, revised 18 October 2018

Accepted for publication 6 November 2018

Published 23 November 2018



CrossMark

Abstract

For cathodic arcs, the cathode material is one of the most important determinants of plasma properties. Consequently, the cathode material—plasma relationship is of special interest in related fundamental research as well as in applications like the synthesis of thin films and coatings. In the latter, the use of multi-element cathodes in inert as well as reactive gas atmospheres is common practice. To further improve the physical understanding of cathodic arcs in such settings, we analyze ions in pulsed cathodic arc plasmas from Nb, Al and two composite Nb–Al cathodes with high time-resolution using a mass-energy-analyzer. The experiments were conducted in Ar atmosphere at total pressures of 0.04, 0.20 and 0.40 Pa, and are compared to earlier results in high vacuum at 10^{-4} Pa. In addition to examining the influence of Ar on ion properties and their cathode material dependence, the results are used to discuss physical concepts in cathodic arcs, like the gas-dynamic expansion of the cathode spot plasma, or the influence of charge exchange collisions of ions with neutrals. While such inelastic collisions e.g. with Ar atoms cause a reduction of charge states to mainly Al^+ and Nb^{2+} at the highest pressure, Ar atoms also seem to take part in near-cathode processes. Ar ions in different time and energy regimes up to 150 eV were observed and compared to Nb and Al ions, showing overlapping velocity distributions for Nb, Al and Ar^+ ions, but also Ar^{2+} ions faster than other ion species.

Keywords: arc discharges, composite cathodes, Ar atmosphere, time-resolved measurements, pulsed arcs, ion charge state distribution, ion energy distribution

(Some figures may appear in colour only in the online journal)

³ Present addresses: Leibniz Institute of Surface Engineering (IOM), Leipzig, Germany, and Felix Bloch Institute, Leipzig University, Leipzig, Germany.

⁴ Author to whom any correspondence should be addressed.



Original content from this work may be used under the terms of the [Creative Commons Attribution 3.0 licence](https://creativecommons.org/licenses/by/3.0/). Any further distribution of this work must maintain attribution to the author(s) and the title of the work, journal citation and DOI.

1. Introduction

Cathodic arcs provide a source of multiply charged metal ions with kinetic energies up to several 100 eV which are used in diverse applications. They find, for example, widespread use in physical vapor deposition for the synthesis of thin films and coatings. There, the utilization of multi-element cathodes and process gases is a necessity to achieve a single plasma stream incorporating all required ions to form homogeneous thin film structures on the substrate with the desired properties. For example, to further improve thermal stability of hard coatings used for cutting tools, complex thin films like Ti–Al–Ta–N [1, 2], Al–Cr–B–N [3] or Cr–Al–Y–N [4] are deposited by cathodic arcs as well as by sputtering techniques using composite cathodes. When using cathodic arcs for such tasks, noble gases are often added in addition to a reactive gas. Even if no reactive gas is needed, the use of a noble gas like Ar on its own is a common practice. Although a gas atmosphere is generally not required for maintaining the arc discharge itself, it is well known that gases like Ar have stabilizing effects on the arc [5], which is why they are frequently used in industrial applications up to a total pressure of several Pa.

One consequence of this development is that concepts of cathodic arc physics, which naturally were built around the simplest case of single-element cathodes in high vacuum, are expanded and more frequently tested on multi-element cathodes [6–10]. There, the applicability of some of these concepts, e.g. the ‘cohesive energy rule’ [11, 12], which states that the arc voltage shows a linear relationship to the cohesive energy of the cathode material, is not trivial. Other concepts, like the ‘velocity rule’, which describes an independence, or weak dependence of the most probable velocity in ion velocity distributions on ion charge states in cathodic arc plasmas [13, 14], have been extended to multi-element cathodes, where for the latter, also ions of the different cathode elements show similar velocities [8]. Furthermore, various studies about the effects of Ar, N or O atmospheres on cathodic arc plasmas from single as well as multi-element cathodes, in particular on metal ion properties, have been published in recent years [15–19]. While ion energy and charge state distributions of cathodic arcs are generally determined in the dense plasma close to the cathode [20] and are related to the cathode material [11], these distributions will change due to interactions with neutral species in the expanded plasma [21]. This is true for arc plasmas at elevated gas pressures, but also in high vacuum. The changes in ion energy and charge state distributions do not only depend on the cathode material, but also on other factors like the length of the plasma stream and chamber geometry [22].

In a previous work, we used an experimental setup providing high time resolution to study how the presence of metal neutrals in the pulsed cathodic arc plasma from composite Nb–Al cathodes alters the plasma properties like ion energy and charge state distributions [23]. Different stages during the arc pulse were identified where the interaction of metal ions with metal neutrals, in particular charge exchange collisions, changes the plasma properties and, hence, confirmed the importance of metal neutrals for cathodic arc plasmas.

As mentioned above, the presence of a background gas like Ar also alters the plasma properties as it represents another source of neutrals that will interact with the expanding arc plasma. In addition, Ar atoms can also participate in the creation of plasma in the cathode spots and, in this way, influence the plasma at its origin. A few studies are available in literature analyzing the effects of Ar on cathodic arc ion properties for Al [15], or composite Ti–Al [19], Cr–Al [18] and Ti_3SiC_2 [17] cathodes using DC arcs as well as pulsed arcs. However, all these studies reported time-averaged data. By applying our experimental setup with high time resolution and using pulsed arcs, we are able to reveal further details about how Ar influences the ion energy and charge state distributions in the plasma. Ar as an inert gas was chosen in order to exclude effects originating from cathode poisoning (compound formation on the surface). An additional factor for selecting Ar was the fact that the Nb–Al cathode model system does not show overlapping in terms of mass-per-charge ratios for the ions of interest, which would have complicated the evaluation of the recorded data. In combination with our previously published results of the Nb–Al cathode model system in high vacuum [23], time-resolved charge and energy distributions of Nb, Al and especially Ar ions in a relevant pressure range will enable us to further discuss related hypotheses in cathodic arc physics, like the ‘velocity rule’ [8], and also improve the understanding of effects induced by a noble gas like Ar in cathodic arcs, which are relevant for applications in physical vapor deposition.

2. Method

The general experimental setup is similar to that of our previous work [23]; a schematic diagram is shown in figure 1. The plasma source used was a ‘self-triggering arc miniature gun’ described in [24], where a cylindrical cathode with a diameter of 6.35 mm and about 20 mm length was mounted. Figure 2 shows the metal plasma gun with a mounted Al cathode in a virgin and eroded state. The cathode materials used were: Nb, Al, and Nb–Al composites with the atomic ratios 75/25 and 25/75. These cathodes were fabricated by powder metallurgical methods using powders with a grain size smaller than 135 μm and ensuring a purity of 99.9%. For every measurement, a virgin or refurbished cathode with a plain and polished surface cleaned with ethanol was mounted and the resistance between anode and cathode was adjusted within the range from 1–500 Ω to ensure reliable ignition of the arc. A conditioning step of about 150 arc pulses was generally carried out before measurements. When signs of arc instabilities due to cathode erosion occurred, measurements were stopped and repeated with a refurbished cathode. The arc miniature gun was positioned in a vacuum chamber of 1 m diameter and 0.25 m height, which was initially evacuated by a scroll pump and then by a cryogenic pump, establishing a base pressure of 10^{-4} Pa. The cylinder axis of the cathode was pointing directly towards the 50 μm diameter orifice of the mass-energy-analyzer (MEA, model EQP300 by Hiden) at a distance of 0.27 m from the cathode. The main components

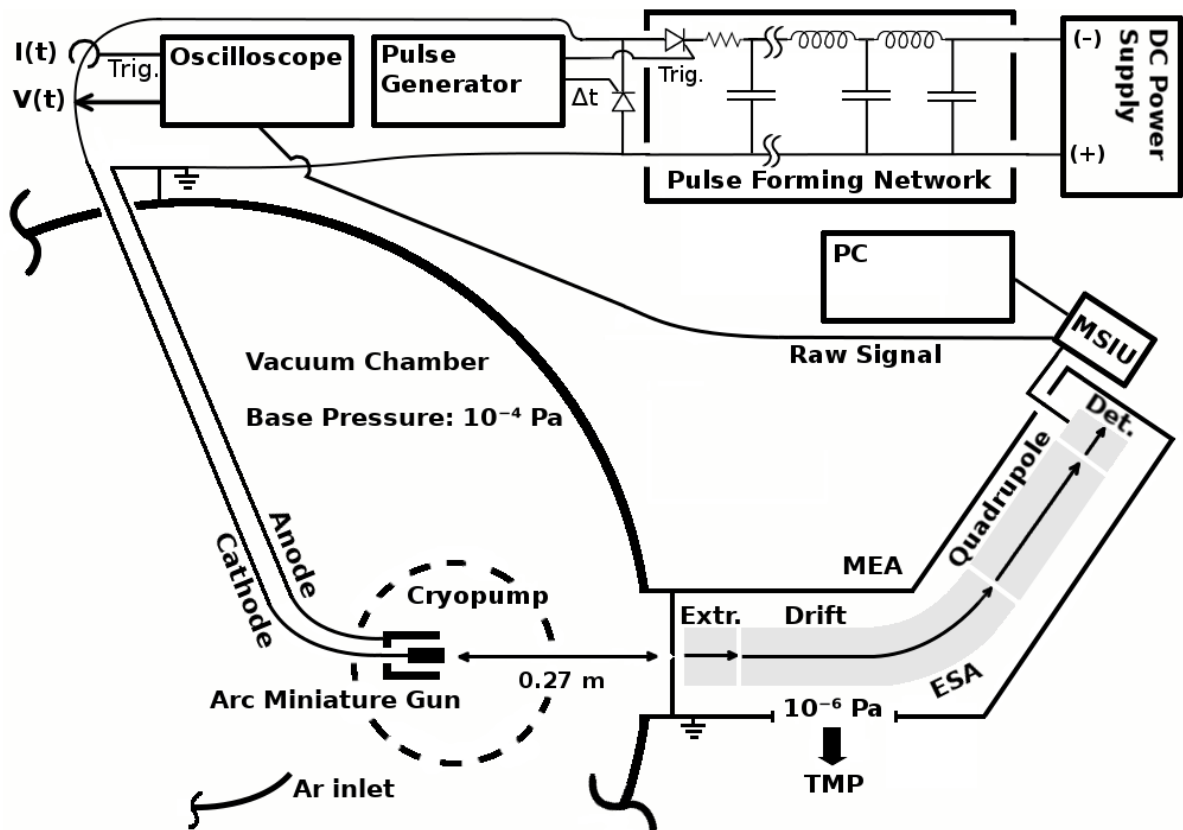


Figure 1. Schematic diagram of the experimental setup, indicating the vacuum chamber with the arc miniature gun as well as the Ar inlet and the valve to the cryo pump; the attached mass-energy-analyzer (MEA), which is differentially pumped by a turbomolecular pump (TMP) and its electronics (MSIU); the electric circuit including a DC power supply, a pulse forming network and a pulse generator; and the instruments used for data processing: an oscilloscope and a personal computer (PC). Further details are explained in the text. Reproduced from [23]. © IOP Publishing Ltd. CC BY 3.0.

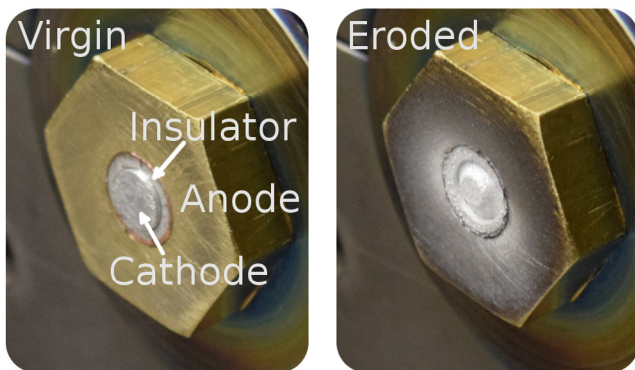


Figure 2. Arc miniature gun with a mounted Al cathode before and after approximately 10^4 plasma pulses. The anode is at ground potential and separated from the cathode by a ceramic insulator.

of this instrument, which was differentially pumped to a base pressure of 10^{-6} Pa by a turbomolecular pump (TMP), were an ion extractor directly behind the orifice (Extr.), an ion drift space followed by a 45° electric sector field energy filter (ESA), a quadrupole mass per charge filter, a secondary electron multiplier (Det.), and the mass spectrometer interface unit (MSIU), which provides the data output to, for example, a personal computer. The detailed properties of the MEA and the parameters used, as well as a brief discussion about the general limitations of plasma analysis based on such a

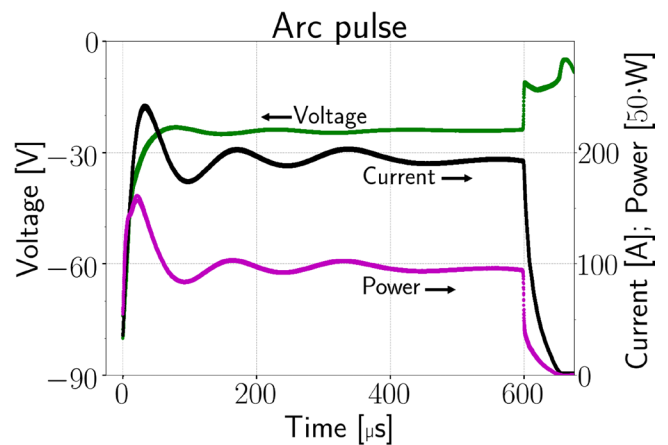


Figure 3. Exemplary time evolution of voltage, current and power of an arc pulse. The shown data was obtained for cathodic arcs from an Al cathode in an Ar atmosphere at 0.04 Pa.

device is given in [23]. Based on the natural abundance of $^{27}_{13}\text{Al}$ (100.0%), $^{93}_{41}\text{Nb}$ (100.0%) and $^{40}_{18}\text{Ar}$ (99.6%) stated in [25], no other isotopes have been taken into account.

To trigger the arc pulse, a 1 kV power supply was charging a pulse forming network (PFN) with 250V, which delivered an approximately rectangular 200 A current pulse of 1 ms. That pulse was prematurely cut-off at 600 μs to enhance its rectangular shape by redirecting the current into a short

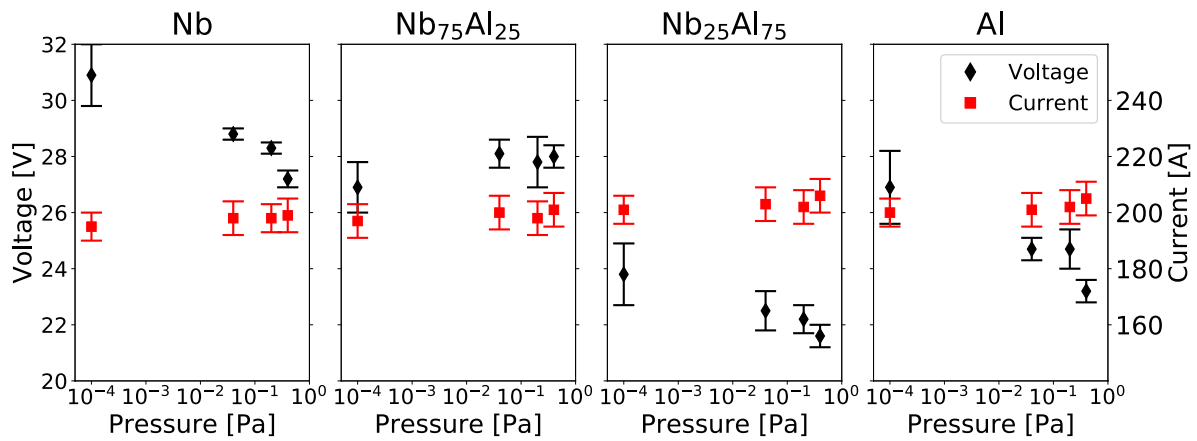


Figure 4. Arc voltage and current in the steady phase of the plasma pulse as a function of the Ar pressure for the different cathode materials. The data points at 10^{-4} Pa originate from a previous experiment described in [23].

circuit, controlled by a pulse generator. These arc pulses were generated four times per second. Voltages and currents were measured directly at the vacuum chamber feedthrough using a 1:100 high voltage probe and a 0.01 V A^{-1} wide-band current monitor. An exemplary time evolution of voltage, current and power of such an arc pulse is displayed in figure 3.

A total pressure of 0.04, 0.2 and 0.4 Pa in the vacuum chamber was realized with an error of 0.01 Pa by balancing the incoming Ar flow with the pumping speed of the cryogenic pump after the base pressure of 10^{-4} Pa had been reached. This was possible by partially closing the valve to the pump and adjusting the Ar flow rate of the mass flow controller (≈ 5 sccm). The latter was calibrated for Ar using the gas correction factor provided in the instrument's manual. The chamber pressure was monitored by a capacitance manometer and a Pirani gauge, as well as by a Bayard-Alpert type ionization gauge; the pressure in the MEA was measured by a cold cathode ionization gauge.

The MEA data output was processed by the instrument's software on a personal computer, as well as directly using an oscilloscope. The latter setup was used in order to drastically improve the time resolution over the one offered by the instrument's software. This was achieved by averaging over 65 oscilloscope acquisitions of similar plasma pulses for each ion energy and charge state. Detailed explanations about this measurement principle can be found in [23, 26]. One oscilloscope acquisition corresponded to a time duration of 1 ms with 10^4 data points (one data point every 100 ns). Each acquisition was triggered by the arc current, recording the signals from the detector as well as those from the voltage probe and current monitor (see figure 1). The energy resolution for time-averaged measurements was 1 eV, while it was decreased for time-resolved measurements to 3 eV for single-charged, 6 eV for double and triple-charged, 8 eV for fourfold and to 10 eV for fivefold charged ions. This change in energy resolution was necessary to keep the duration of the experiments within reasonable time frames. The voltage signal of the MEA detector was corrected by its offset of about 4.9 V and in addition by its own background (after the signal showed no significant detections but background only) for each separate measurement. The resulting voltage is proportional to the

ion counts and referred to as 'intensity', a naming convention introduced in [26]. This 'intensity' has the unit 'volt', because it is an average of the detector voltage over 65 similar plasma pulses. The time-resolved data were further corrected by the ions' time of flight inside the MEA [23]. The energy change of the ions in the plasma sheath to the grounded MEA orifice, however, was not corrected. The experimental results reflect the state at the grounded MEA orifice. A discussion about this decision, as well as detailed explanations regarding time correction and intensity can be found in [23].

3. Results

The observed plasma pulses generally show a transient behavior right after triggering, which then transitions into a steady phase, typically reached after 100–300 μs . Another transient phase starts right after the cut-off at 600 μs . The results will frequently show data time-integrated from 300 to 500 μs , which will be referred to as 'the steady phase' of the plasma pulse. The use of other time intervals will be explicitly mentioned.

3.1. Arc current and voltage

The measured voltages and currents for every cathode material are displayed in figure 4 for the steady phase of the plasma pulse, for different Ar gas pressures. The voltage drops inside the cathode and other relevant parts of the circuit were not corrected. Each data point shows an average of all corresponding voltage and current samples. The cathode erosion and the formation of a metal film on the insulator between cathode and anode leads to a slight decrease of voltage proportional to the number of pulses and, in addition to the intrinsic voltage fluctuations of cathodic arcs [27], to large uncertainties. The error bars in figure 4 only indicate a lower limit of the standard error. Nevertheless, the known cathode material—voltage characteristics for Nb–Al cathodes in high vacuum [23] are in general still preserved in Ar atmosphere: the Nb₂₅Al₇₅ cathode shows the lowest voltages, followed by Al, Nb₇₅Al₂₅ and the Nb cathode. Further, with the exception of the Nb₇₅Al₂₅

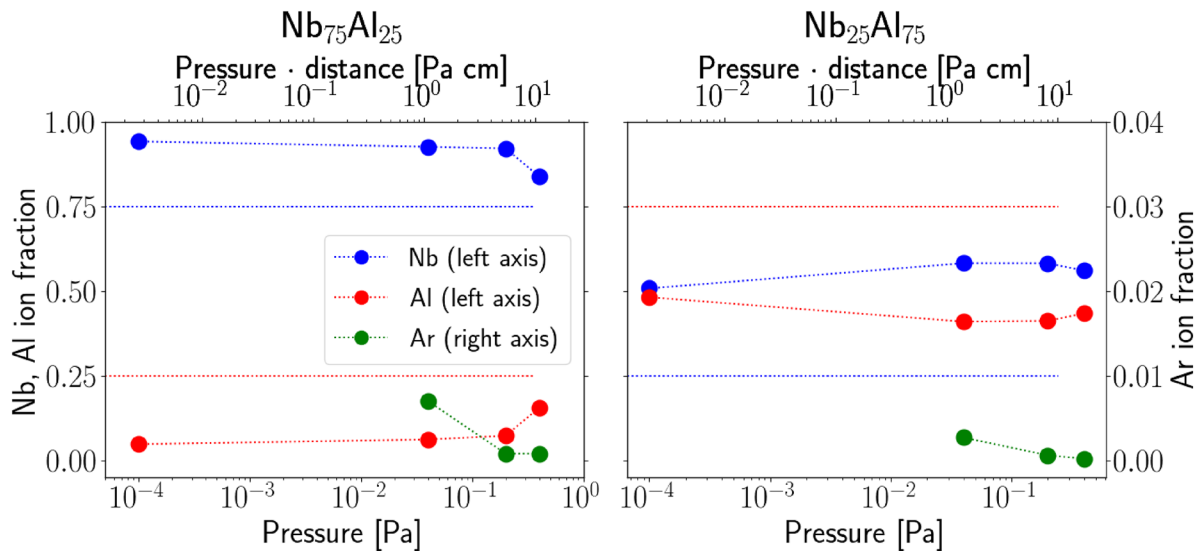


Figure 5. Elemental fractions of detected ions of $\text{Nb}_{75}\text{Al}_{25}$ and $\text{Nb}_{25}\text{Al}_{75}$ cathodes depending on pressure, for the steady part of the plasma pulse. The Ar fractions are shown in a different scale (right axis). The chemical composition of the cathode is indicated by blue (Nb) and red (Al) horizontal lines (applying to left axes). The data points at 10^{-4} Pa originate from a previous experiment described in [23].

cathode, a trend of decreasing and less fluctuating voltages with increasing Ar pressure is noticeable. The currents remain relatively constant around 200 A, because the total impedance is dominated by the PFN and not the arc discharge.

3.2. Plasma composition

The fractions of Nb, Al and Ar ion intensities depending on pressure are shown in figure 5 for the two composite cathodes. The data was obtained for the steady part of the plasma pulse. The dotted horizontal lines indicate the corresponding Nb–Al fractions in the cathode. The Ar ion fractions are all below 1%. Compared to the cathode Nb–Al fractions, about 20% more Nb and less Al ions were detected in the plasma, which changes only marginally with increasing Ar gas pressure.

3.3. Ion energy and charge state distributions

A visualization of the recorded intensities from the $\text{Nb}_{75}\text{Al}_{25}$ cathode is shown in figure 6 as an example. It displays the ion intensities depending on their kinetic energy at the MEA orifice, the time after triggering the arc, their charge state and elements (rows), and the variation with different pressure in the chamber (columns). The basic shape and properties of such pulses is already described in [23, 26]. A general increase of lower and decrease of higher charge states, as well as a shift to lower energies can be observed with increasing Ar pressure. For the cathode composition shown, no significant detections were found for higher charge states than those shown in the figure. The highest observed charge states including all cathode materials were: Nb^{5+} , Al^{3+} and Ar^{2+} . Similar intensity–energy–time datasets for the observed charge states at these pressures were obtained for the $\text{Nb}_{25}\text{Al}_{75}$ cathode as well as for the Nb and Al cathodes.

For the steady phase of the plasma pulse, ion charge state fractions and average charge states depending on pressure and

cathode material are shown in figure 7 for Nb and Al ions. The charge state fraction is calculated by dividing the energy-integrated intensities of Nb or Al ions by the sum of the energy-integrated intensities of all charge states of the corresponding element. A quantitative expression used for these calculations is provided in equation (4) in [23]. While increasing Ar pressure leads to a decrease of average charge state of Al ions to about 1, the Nb ions' average charge state reduces only to about 2. In contrast to the Al ions, the Nb ions' average charge state also shows a slight cathode material dependency. At the highest pressure of 0.4 Pa, mainly Nb^{2+} and Al^{1+} ions are detected.

3.4. Ar ions

Although the fraction of Ar ions is less than 1%, the absolute intensity of Ar ions is enough to investigate these ions in detail. To give an example, figure 8 provides a visualization of the Ar ion intensities for the Nb cathode. Only in the arc plasma from this cathode, significant intensities of Ar^{2+} ions were recorded. Substantial intensities of low energy Ar ions following the cut-off were observed, continuing for several hundred microseconds (extending over the range shown in figure 8). A consequence of these ions to the Ar^+ energy distributions can be seen in figure 9, again for the Nb cathode. There, a time-averaged measurement utilizing the instrument's standard software (red triangular data points) is compared to time-resolved data integrated over two different time intervals: from 300 to 600 μs (green) and 0 to 600 μs (blue). While the time-averaged data only shows low energy Ar^+ ions increasing with pressure, a transition from high to low energy Ar^+ ions with pressure can be observed for the time-resolved data when excluding detections after the cut-off. The latter is further analyzed for all cathode materials by a comparison of the cumulative Ar ion intensities in the first 600 μs of the pulse, which is displayed in figure 10 for the different Ar gas pressures. It shows Ar^+ and Ar^{2+} ion intensities for this time

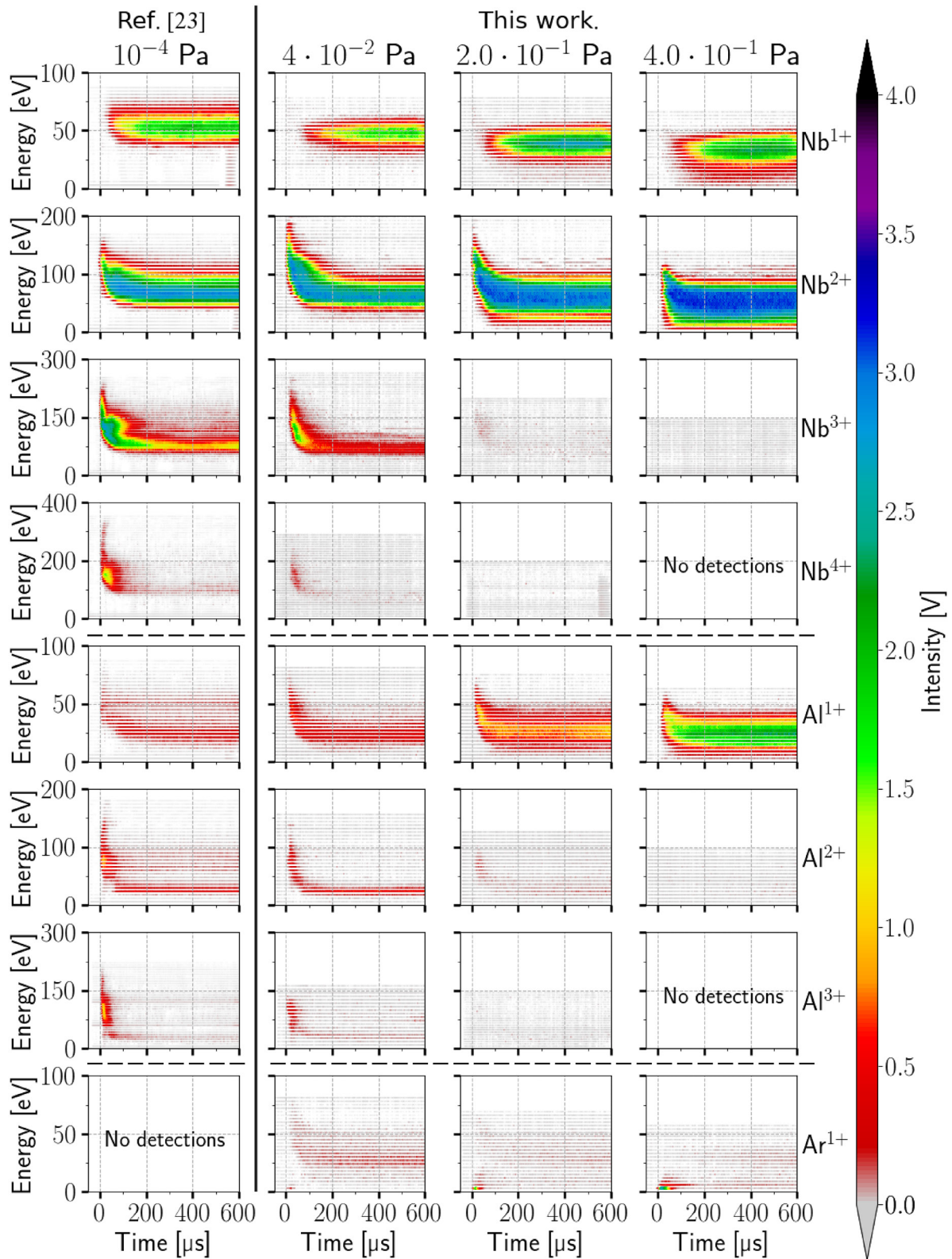


Figure 6. Intensities of Nb, Al and Ar ions from a Nb₇₅Al₂₅ cathode depending on the time after triggering the plasma pulse, on their kinetic energy at the MEA orifice, on their charge state (rows), and on the total pressure in the chamber (columns). The data at 10⁻⁴ Pa originates from a previous experiment described in [23].

interval and for two energy intervals: 0–20 eV (a) and 20 eV up to the highest observed energy (b). These energy intervals were chosen based on the Ar ion energy distributions and with the energy resolution of 3 eV for single and double charged

species in mind. According to this figure, the reduction of the higher energy Ar⁺ ions with increasing pressure is confirmed. It also shows that the reduction is stronger for cathodes with higher Al contents. The Ar²⁺ ions mainly show high energies

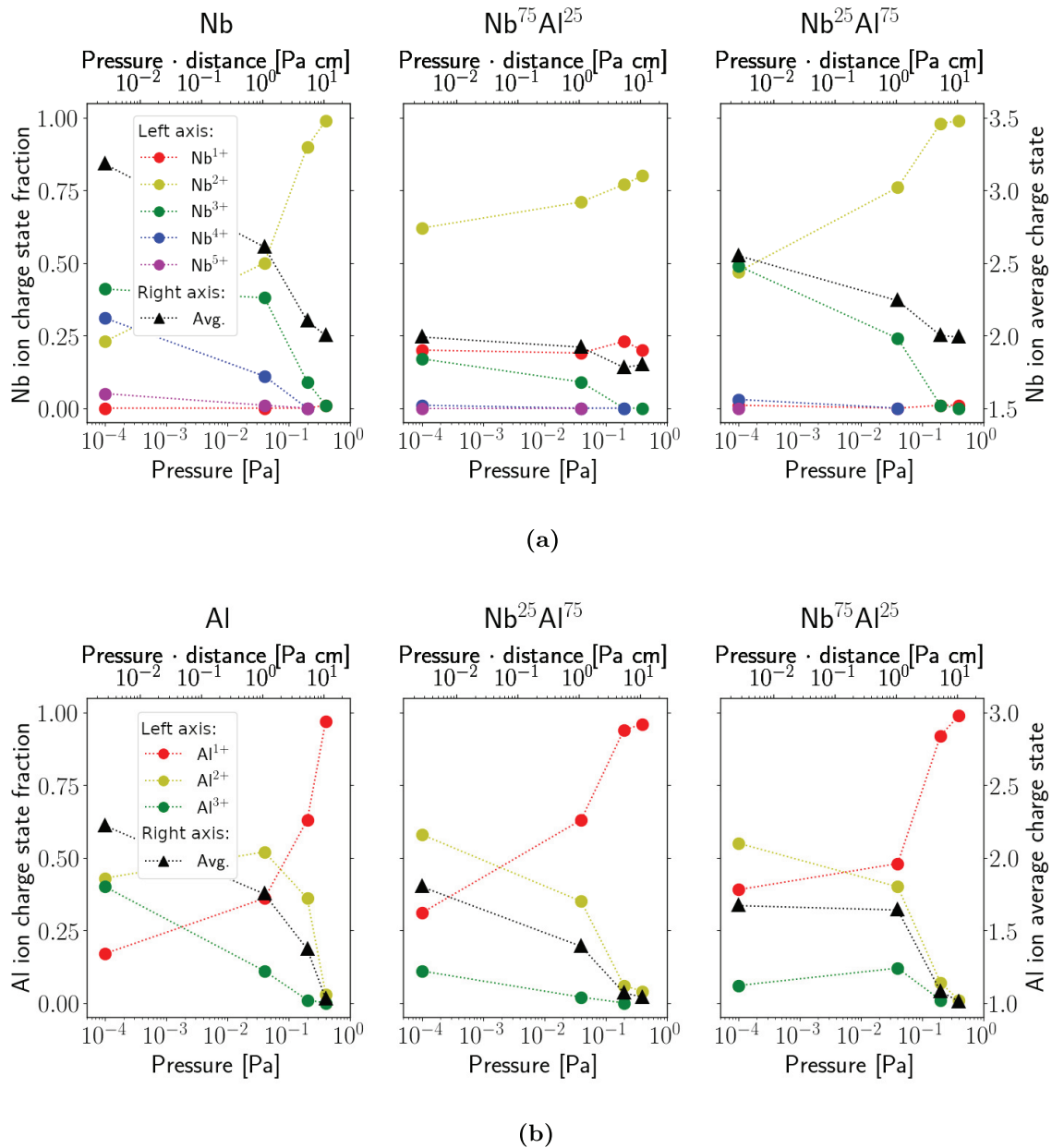


Figure 7. Charge state fractions (colored, left axis) and average charge states (black, right axis) of (a) Nb and (b) Al ions depending on pressure and cathode material. The data shown is based on intensities for the steady phase of the plasma pulse and energy-integrated over the whole energy range. The data points at 10⁻⁴ Pa originate from a previous experiment described in [23]. (a) Nb ions. (b) Al ions.

and their cumulative intensity increases with increasing pressure. The low energy ions only show a distinct increase for the Nb-rich cathodes: Nb₇₅Al₂₅ and Nb.

3.5. Ion velocities

All ion velocities (v) in the current work have been calculated directly from kinetic ion energies (E_k) and masses (m) using equation (1) and reflect the situation at the grounded MEA orifice.

$$v = \sqrt{\frac{2E_k}{m}}. \quad (1)$$

Even though Ar ion intensities are lower by an order of magnitude compared to Nb and Al ions, their velocity distributions are clearly distinguishable from noise and can be compared to others, in particular at the lowest pressure of 0.04 Pa. Figure 11 displays such a comparison between ion velocity distributions of the differently charged Ar, Al and Nb ion species for the total pressure of 0.04 Pa in the steady phase of the plasma pulse. The general cathode material dependency, which was already observed in high vacuum measurements in [23], is also present in an Ar atmosphere at 0.04 Pa: ions from composite cathodes show generally lower velocities than from single-element cathodes and ions from the Nb₇₅Al₂₅ cathode show lower velocities than ions from the Nb₂₅Al₇₅ cathode.

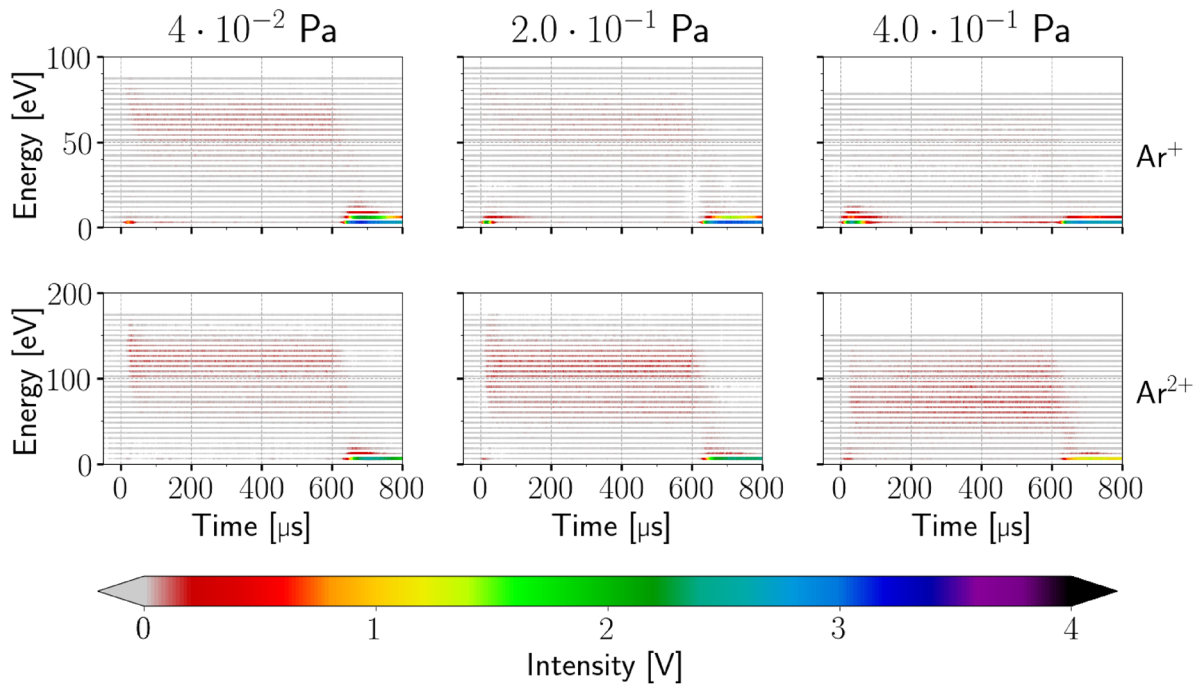


Figure 8. Energy and time dependent intensities of Ar ions for the Nb cathode, showing the observed charge states (rows) at three different Ar pressures (columns).

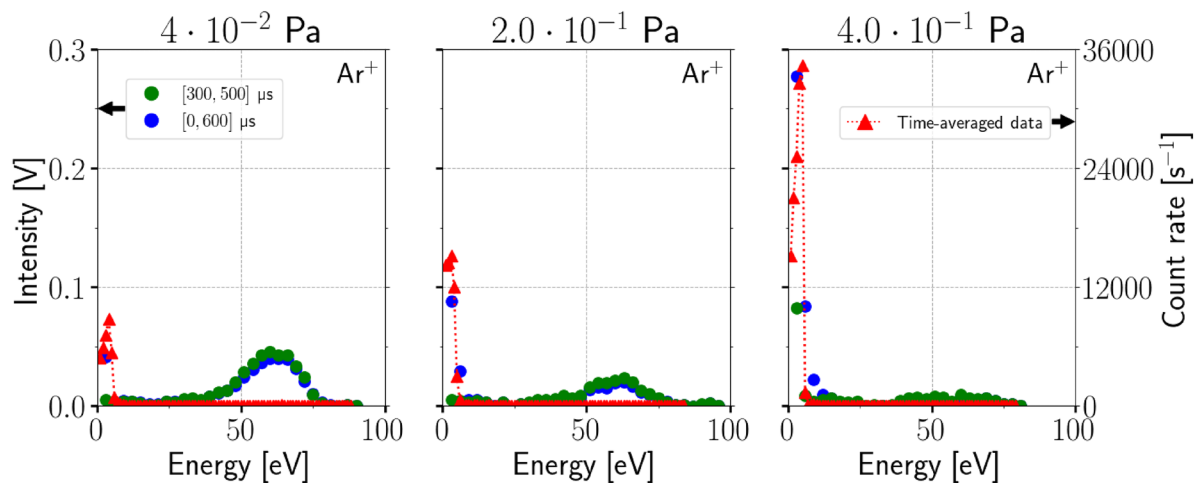


Figure 9. Energy distributions of Ar⁺ ions depending on pressure for the Nb cathode. In addition to data time-integrated from 300 to 600 μs (green) and 0 to 600 μs (blue), time-averaged data is plotted in red.

Furthermore, only a moderate dependency of the most likely ion velocities (peaks of the distributions) on ion charge state and element is visible. With exception of the Ar²⁺ ions of the Nb cathode, the Ar ion velocity distributions are similar to the metal ions, in particular when compared to Nb ions.

Based on the observed ion charge states at the highest Ar pressure, mainly Nb²⁺ and Al⁺, the velocity distributions of these two ion species are additionally visualized in figure 12 for the steady part of the plasma pulse, showing all Ar pressures (colors) and cathode materials (columns). A general shift to lower velocities with increasing Ar pressure can be observed and a substantial increase of the lowest velocities of Al⁺ ions from the Al cathode at 0.40 Pa.

4. Discussion

4.1. Arc voltage

One of the most important parameters of cathodic arcs, the burning voltage, has been extensively analyzed in the literature of vacuum arcs, e.g. in [12, 28, 29], and its cathode material dependency is well documented [11]. Information on its pressure dependency for different gas species, however, is rather sparse. Zhirkov *et al* [19] reported a decrease from 21 V to 17–18 V for composite Ti–Al cathodes, when comparing their results at a base pressure of 7×10^{-4} Pa to those obtained at 4 Pa Ar atmosphere. In our case, the voltages for

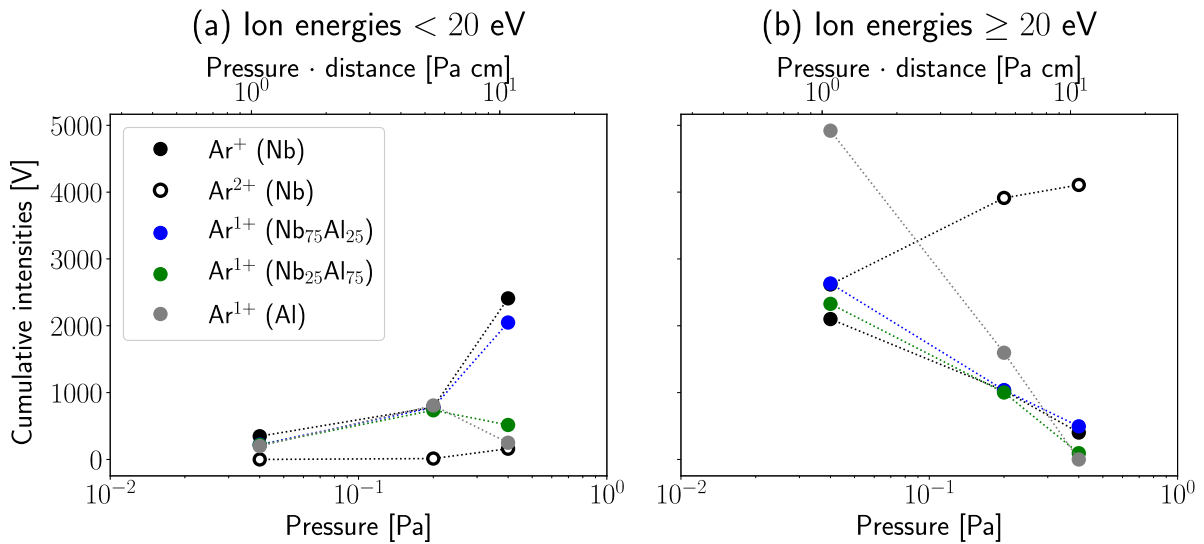


Figure 10. Cumulative Ar ion intensities in the first 600 μs of the pulse for two different energy intervals: (a) less than 20 eV and (b) greater than or equal to 20 eV. The results for the four different cathodes are differentiated by colors.

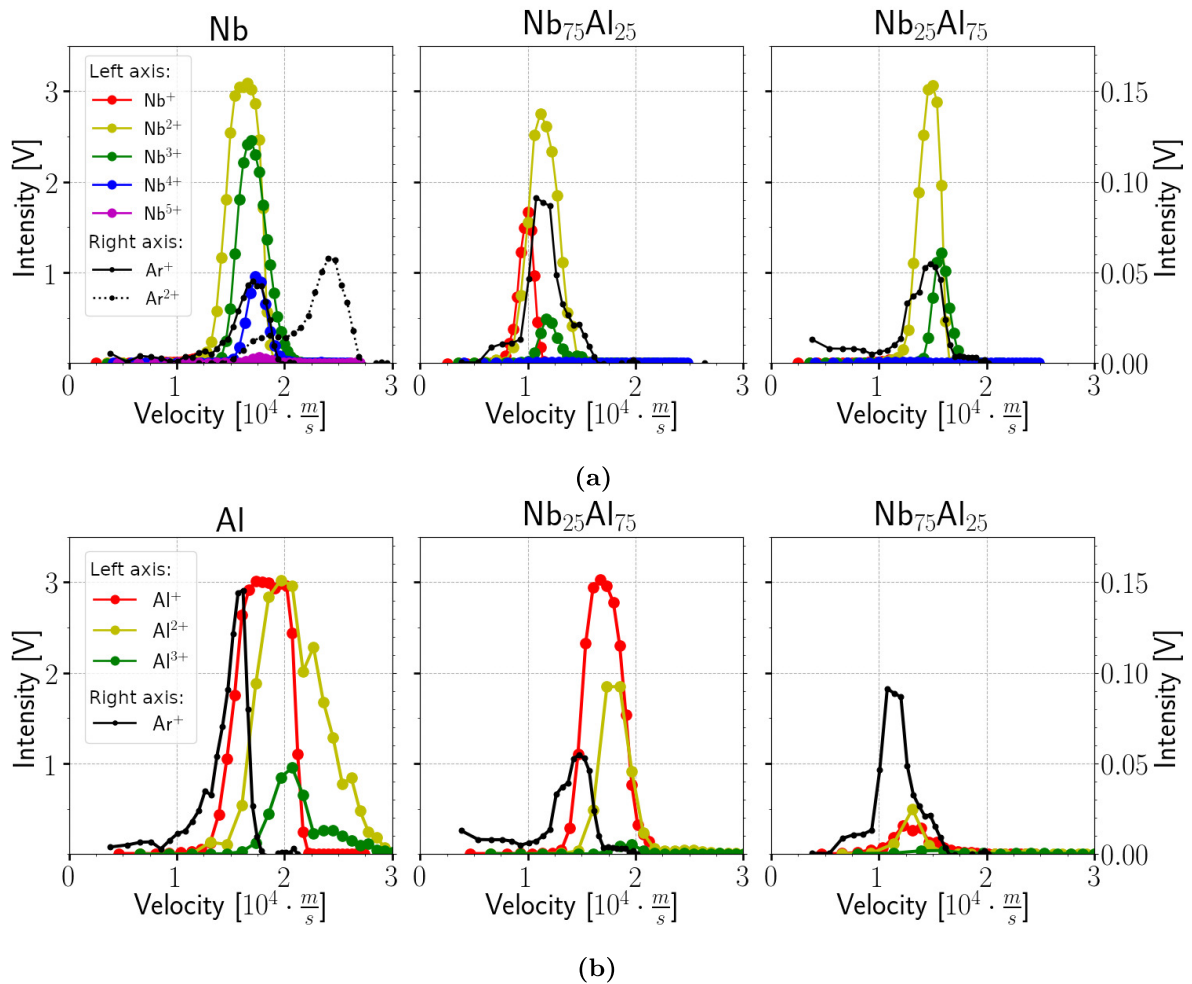


Figure 11. Ion velocity distributions for Ar ions compared to (a) Nb and (b) Al ions for all observed charge states at a total pressure of 0.04 Pa for the steady phase of the plasma pulse. The ion intensities are shown in two different intensity scales: the left axis applies to Nb and Al ions, while the right axis applies to Ar ions.

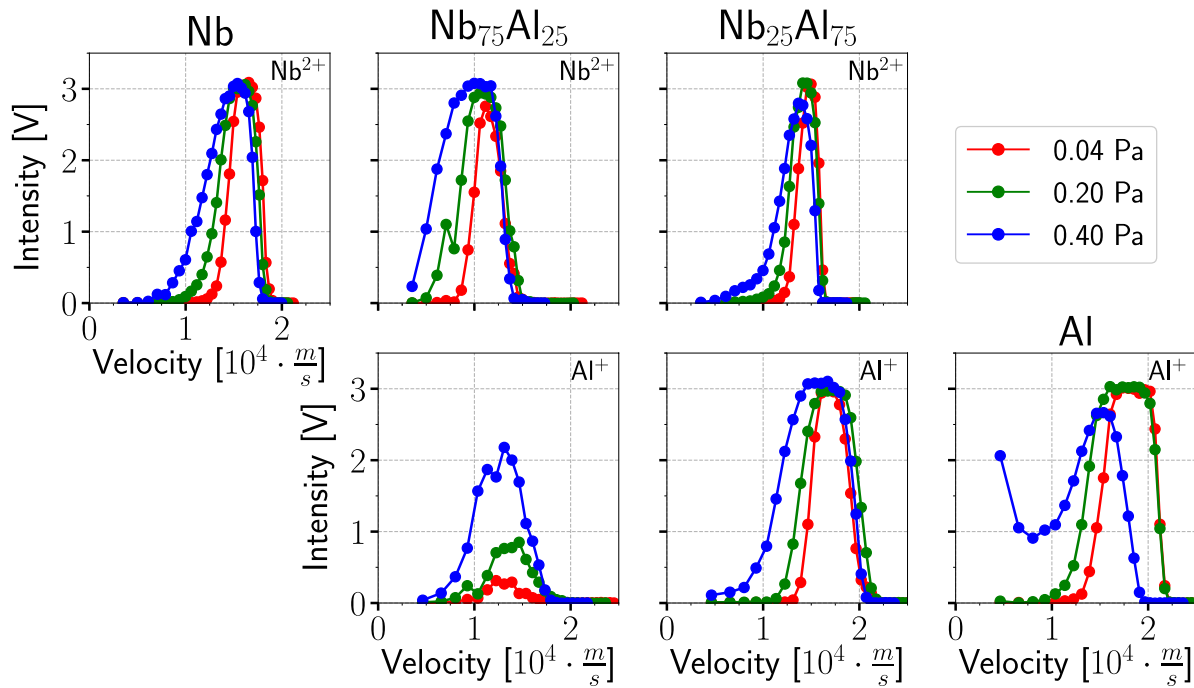


Figure 12. Velocity distributions of Nb^{2+} (1st row) and Al^+ (2nd row) ions depending on Ar pressure (colors) and cathode material (columns), for the steady phase of the plasma pulse.

the Nb–Al cathode model system in high vacuum [23] compared to the present results in an Ar atmosphere show a similar trend. The material dependencies are still present and voltages decrease with pressure for all cathode materials, except for the $\text{Nb}_{75}\text{Al}_{25}$ cathode composition. The voltage decrease is most likely related to an increased likelihood of spot ignition due to the presence of Ar. Potentially, that leads to further ions impinging the cathode surface and creating secondary electrons which are then accelerated in the arc voltage drop [5]. Furthermore, these voltage dependencies are a direct indication of an involvement of Ar atoms in cathode spot processes.

4.2. Steady-state plasma composition

For the composite cathodes, the fractions of detected Nb, Al and Ar ions are shown in figure 5. Just a slight influence of Ar pressure is observable, particularly at the highest pressure of 0.4 Pa. The general discrepancy of the Nb–Al ratio in the cathode compared to the Nb–Al ratio of the detected ions was already discussed in [23] and is likely to be caused by different angular distributions of light (Al) and heavy (Nb) elements in cathodic arcs of composite cathodes [9]. A general deficiency of lighter ions in cathodic arcs of composite cathodes is frequently observed, e.g. in [9] for ZnPb cathodes, in [7] for TiSiC cathodes and in [17] for TiSi cathodes. In the latter, the authors also compared different Ar pressures and reported a slight decrease of this effect from about 0.01–10 Pa cm and an increase for greater values up to about 70 Pa cm of the pressure distance-product. In the current results, one can also see a slight decrease of the Al ion deficiency when comparing the ion fractions at 5.4 and 10.8 Pa cm.

4.3. Ion charge states of Nb and Al ions

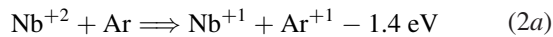
A substantial reduction of average ion charge states and energies in the expanded plasma is a frequently observed influence of an added background gas in the cathodic arc vacuum chamber [15–19] and a consequence of the increased ion-gas interaction at higher pressures. Depending on gas type and cathode material, there is typically a critical pressure-distance product where these effects start to appear. For example, for Al cathodes, effects on average charge states have been observed to start at about 0.5 Pa cm [16] and to saturate at 10–30 Pa cm [15, 16], where the commonly observed charge states up to Al^{3+} shift to Al^+ only. A simple model (a mixture of two gases) to estimate the thermal mean free path (MFP) for Ar and another element, like, for example, Ti was applied in [17]. The results show that in this pressure-distance range, the MFP estimate shortens by nearly two orders of magnitude to a few centimeters. That fits the observed reduction of average charge states when considering charge exchange collisions with Ar and the typical length of the plasma stream, which is usually at least 10 cm.

In the current work, the results cover pressure-distance values ranging from 1 Pa cm to 11 Pa cm in addition to reference values of 2.7×10^{-3} Pa cm. When analyzing these results over a steady part of the plasma pulse (from 300 to 500 μs), a decrease of average charge states with pressure is generally observable for Nb as well as Al ions in figure 7. While the detected Al ions shift to nearly exclusively single charge states at the highest pressure of 0.4 Pa, the Nb ions show a different behavior: increasing Nb^{2+} ions with Ar pressure. With the exception of the $\text{Nb}_{75}\text{Al}_{25}$ cathode, mainly

Table 1. Cumulative ionization energies (E_{ci}) of Nb, Al and Ar atoms [25] up to relevant charge state numbers (Q).

Q	E_{ci} (eV)		
	Nb	Al	Ar
1	6.76	5.99	15.76
2	21.08	24.81	43.39
3	46.12	53.26	84.13
4	84.42		
5	134.97		

double-charged Nb ions were detected at 0.4 Pa. Although it is known that for high vacuum cathodic arcs of Nb or Ta cathodes, only very low fractions of single-charged ions are generally detected (e.g. 1% Nb⁺ and 2% Ta⁺ in [30], 0% Ta⁺ in [31] or 0% Nb⁺ in [23]), in an Ar environment one would still expect a reduction of Nb²⁺ to Nb⁺ ions by charge exchange with Ar atoms. That is, however, not observed in the current results. There are various side effects which can affect the fraction of detected Nb⁺ ions, e.g. a generally decreased detection of single-charged species due to angular distributions of ion properties [32, 33]. However, a more likely explanation seems to be the lack of feasible charge exchange reactions. When considering the two ion-atom collisions in equation (2) and the relevant ionization energies in table 1, the potential energy difference between the initial and final states (ΔE) of the reaction is positive for equation (2b), while it is negative for equation (2a). For the present ion velocities in the order of 10⁴ m s⁻¹, a positive ΔE is required for appreciable cross sections [34], which is in line with the observed dominance of Nb²⁺ and Al⁺ charge states at 0.4 Pa.



The significantly increased fraction of Nb⁺ ions in the plasma of the Nb₇₅Al₂₅ cathode was already observed for Nb₇₅Al₂₅ and Nb₆₇Al₃₃ composite cathodes in high vacuum in a previous work [23]. The current results show that these Nb⁺ ions do not depend on Ar pressure and lead to a slightly lower average charge state of 1.8 at 0.4 Pa for this cathode material (see figure 7(a)). This observation is in agreement with theoretical considerations, where charge exchange collisions between Nb⁺ ions and Ar atoms are considered to have low cross sections due to a negative ΔE (compare ionization energies of Nb and Ar atoms in table 1). The occurrence of Nb⁺ ions is just one example of the material dependencies within the used cathode model system. It is known that for the current Nb–Al cathodes in high vacuum, ion charge states are quite material dependent initially, and charge exchange collisions with Nb and Al neutrals further change the charge state fractions up to 300 μ s into the pulse [23]. At a low pressure range, 0.04–0.2 Pa, these effects still have a large impact in the current results. That can be seen exemplarily for the Nb₇₅Al₂₅ cathode in figure 6, where, when compared to high vacuum, the typical shape of the pulses (which is also a characteristic of occurring charge exchange collisions) only slightly changes at an increased pressure of 0.04 Pa. Also figure 7(a) clearly

reveals this influence when looking at the material dependency of charge states for low pressures. Since these results reflect the middle, steady part of the plasma pulse, they already incorporate the known material dependent initial charge states as well as the different charge exchange characteristics in the first part of the pulse [23], which leads to the different starting points of average charge states at 0.04 Pa in figure 7. However, at 0.4 Pa the charge states are equalized and no more material dependencies apart from the modest influence of Nb⁺ ions in the plasma from the Nb₇₅Al₂₅ cathode are observed.

4.4. Ar ions: steady-state versus transient plasma regimes

Time-resolved data makes the analysis and comparison of separate parts of the plasma pulse possible, that means Ar ions can be examined in transient as well as in the steady-state regimes. Although the measured ion ‘intensities’ do not provide absolute numbers of the detected Ar ions, they can be used to qualitatively compare different intensities. When only considering the steady-state plasma like in figure 5, the fraction of Ar ions is less than 1% and shows a decrease with Ar pressure. A decrease of Ar ions with pressure was also observed in [17], as well as in [33] and explained by a decreased chance of Ar ions reaching the detector when considering decreasing kinetic energies and MFP of Ar with pressure [17]. The authors of [33] argued that the angular Ar ion distribution is more isotropic at higher pressure, which could also lead to a decrease of Ar ion detections with pressure when detecting on-axis (like in the present work). A closer look on the Ar ion intensities in figure 8 reveals two different energy regimes: fast Ar ions with kinetic energies comparable to those of Nb and Al ions up to 150 eV, and relatively low energy Ar ions with kinetic energies less than 20 eV. In the transient parts of the pulse, especially directly after trigger and cut-off, the intensities of low energy ions are generally increased, possibly indicating more frequent charge exchange reactions. The material-dependent behavior of the cumulative Ar⁺ ion intensities with increasing pressure in figure 10(b) might also be related to a dominance of different charge exchange reactions. Apart from the general decrease of high energy Ar⁺ ions, figure 10(a) also shows increasing low energy Ar⁺ ions when comparing 0.04 and 0.2 Pa. However, comparing 0.2–0.4 Pa shows a strong increase of low energy Ar⁺ ions for Nb-rich cathodes, and a slight decrease for Al-rich cathodes. A higher Nb fraction in the cathode seems to promote low energy Ar ions, which mainly appear directly after triggering (see figure 8). That might be related to the higher maximum charge states of Nb ions, which in principle provide a larger variety of charge exchange reactions with Ar atoms up to Nb⁵⁺. Another ionization mechanism producing low energy Ar⁺ ions is electron impact ionization, which might be increased for Nb-rich cathodes, which typically also show higher electron temperatures [35] in the near-cathode plasma. A similar trend was observed in [19], where cathodic arcs of Ti–Al cathodes in Ar atmosphere also displayed a material dependent increase/decrease of Ar ions when increasing the pressure from about 0.07 to 0.7 Pa: high Al fractions in the cathode led to a decrease, while high Ti fractions led to an

increase of the Ar ions, whose majority was detected with low kinetic energies.

4.5. Ion velocity distributions

4.5.1. The velocity rule. Various experiments with cathodic arcs demonstrated that the peaks in ion velocity distributions do not, or only slightly, depend on ion charge state and element [8, 14, 36], which is known as the ‘velocity rule’ [8]. This supports the hypotheses of a gas-dynamic expansion of the cathode spot plasma. In this picture, the different ion species are accelerated collectively within ‘microexplosions’ at the cathode and then move at similar velocities [37]. A theoretical model based on ion–ion coupling in the high density plasma at the cathode also predicts this behavior, but likewise moderate relative velocities up to 10–15% of the average jet velocity [38]. For our Nb–Al model system in high vacuum, a similar behavior was observed and moderate deviations up to 15% were detected. When comparing the ion velocity distributions for Nb, Al and Ar ions in the current work at 0.04 Pa (figure 11), it can be noticed that the velocity distributions of Ar⁺ ions are within those of Al and Nb ions, in particular when compared with Nb ions in figure 11(a). These high energy Ar ions could be accelerated in two different ways: together with Nb and Al at the cathode, or by charge exchange collisions initiated by Nb and Al ions in the expanded plasma. For the latter, one would expect lower Ar ion velocities compared to Nb or Al ions, depending on ion masses, collision angle and energy defect. The relatively good match of ion velocity distributions of single-charged Ar ions compared to Nb and Al ions points towards the first hypothesis.

4.5.2. The velocity mismatch of Ar²⁺ ions. For the Ar²⁺ ions, which have only been detected for the Nb cathode in significant quantities, a different behavior in figures 10 and 11(a) can be observed. We found higher velocities compared to the other ion species and also slightly increasing intensities with pressure; both are unusual. Although the Ar²⁺ ion velocity distribution shows a shoulder in the vicinity of the velocity distribution maxima of the other ion species in figure 11(a), its maxima is not in line with the velocity rule. Strictly speaking, Ar²⁺ ions were not detected, but ions with a mass-per-charge ratio of 20 u e⁻¹ (where ‘u’ is the unified atomic mass unit and ‘e’ the elementary charge), which leaves the possibility that other ion species with very similar mass-per-charge ratio might interfere with the recorded signal. However, a mass-per-charge ratio of (20.0 ± 0.5) u e⁻¹ is required for significant intensities, which can only be realized by ion masses which are near a multiple of 20 u. The assumption of an ion with a mass of 20 u does not lead to decreased velocities. The next iteration of 40 u corresponds to Ar²⁺. Each further mass increase by 20 u requires, again, an increased charge state, which will consequently, increase the energy scale. Furthermore, very high charge states like +10 and higher can be ruled out for energy reasons. Therefore, no additional ion species can be identified, which would shift the velocity distribution to lower values, matching other observed ions, while satisfying a mass-per-charge ratio near 20 u e⁻¹. As a result, it is concluded that indeed Ar²⁺ ions are observed, but

the mechanisms responsible for their energy gain are unclear as their higher velocity suggests an acceleration outside the cathode spot vicinity, and in addition to the acceleration during the expansion of the cathode spot plasma.

4.5.3. Nb and Al ion velocity distributions. The ion velocity distributions of Nb and Al ions show pressure dependencies, which are displayed in figure 12, exemplarily for the ions most prominent in Ar atmosphere: Nb²⁺ and Al⁺. A general trend is an asymmetric broadening of the velocity distributions at low velocities. That can be understood by the increased amount of detected ions which lost kinetic energy due to previous inelastic or elastic collisions. While this leads to decreased average ion energies, the maxima of the ion velocity distributions only change marginally. The Al cathode slightly differs from the others, showing increased Al⁺ ions at the lowest velocities and also a stronger decrease at high velocities, when compared to the Nb₂₅Al₇₅ and Nb₇₅Al₂₅ cathodes. This might be related to the charge exchange reaction in equation (2b), but the same effect should then also be visible for the other cathode compositions. Furthermore, a similar behavior of the Nb²⁺ ions due to charge exchange reaction equation (3) would be expected.



$$E_1/E_2 = \frac{4m_1m_2}{(m_1 + m_2)^2} \cos^2 \theta. \quad (4)$$

Another possible explanation is the different energy transfer from ions to Ar atoms in elastic collisions, where Al ions transfer more energy due to the smaller mass difference between the collision partners. The energy transfer between two atoms in an elastic collision is given in equation (4), where E is the kinetic energy, m the mass and θ the collision angle. It is maximal if the collision partners have equal masses and the collision angle θ is 0 or 180°. The maximum energy transferred from a Nb ion to an Ar target atom is 84%, while it is 94% for an Al ion. Also, a potentially higher amount of Al neutrals when using a pure Al cathode could lead to ionization of Al atoms by Ar⁺ ions, which would provide another source of low energy Al⁺ ions and decrease cumulative Ar⁺ intensities, like in figure 10(a) at 0.4 Pa.

5. Conclusions

The time-resolved analysis of ion properties in pulsed cathodic arc plasmas from Nb, Al and composite Nb–Al cathodes depending on Ar pressure leads to the following conclusions:

The known cathode material—voltage characteristics for Nb–Al cathodes in high vacuum [23] are still preserved in an Ar atmosphere up to 0.40 Pa: the Nb₂₅Al₇₅ cathode shows the lowest voltage, followed by Al, Nb₇₅Al₂₅ and Nb cathodes. A trend of decreasing and less fluctuating voltages with increasing Ar pressure, which is most likely related to an increased likelihood of spot ignition due to the presence of Ar, was observed. Also, the steady state plasma composition is only marginally influenced by a pressure increase up to 0.40 Pa. Compared to the cathode composition, the plasma

generally shows a deficiency of Al ions of about 20% for composite cathodes, which is likely to be related to angular distribution of ions, and an Ar ion fraction of less than 1%.

The highly material-dependent distribution of ion charge states for the steady state regime of the plasma pulse in high vacuum (with charge states up to Nb^{5+} and Al^{3+}) shifts to almost only Nb^{2+} and Al^+ ions at 0.40 Pa, drastically reducing the influence of the cathode material. The latter is explained by interaction of Nb and Al ions with Ar atoms in form of charge exchange collisions, which is strongly increasing in the pressure-distance interval from 1 to 11 Pa cm. The presence of mainly Nb^{2+} ions is unusual when compared to other studies, where increasing Ar pressure ultimately leads to single-charged species for various materials [15–19]. It can be attributed to a low cross section of the related Nb^{2+} —Ar charge exchange collision due to a negative energy defect. The velocity distributions of these remaining Nb^{2+} and Al^+ ions show an asymmetric broadening at low velocities, when compared to lower Ar pressures of 0.04 and 0.20 Pa, which can also be understood by the increased amount of detected ions which lost kinetic energy due to previous inelastic and elastic collisions.


The signal of Ar ions is generally dominated by high intensities of low energy single-charged ions (≤ 20 eV) appearing after the cut-off (≥ 600 μs). A focus on the first 600 μs of the plasma pulses reveals the presence of Ar^+ ions with high kinetic energies up to 100 eV, which show quite similar velocities compared to Nb and Al ions. This points to a collective acceleration of Ar with other species within microexplosions at the cathode. With increasing Ar pressure, these fast Ar^+ ions are fading for all cathode materials, while the flux of slower Ar^+ ions is increasing particularly after triggering the plasma pulse, depending on the Al content in the cathode. However, when using the Nb cathode, also Ar^{2+} ions with very high kinetic energies up to 150 eV were detected. Their velocity is clearly higher compared to other ion species, which suggests an acceleration outside the cathode spot vicinity, and in addition to the acceleration during the expansion of the cathode spot plasma. To fully understand this behavior, further research is needed.

Acknowledgments

This work was supported by the Austrian Science Fund (FWF, Project No. P 27867-N36). Work at LBNL was supported by the US Department of Energy under Contract No. DE-AC02-05CH11231.

ORCID iDs

Siegfried Zöhrer  <https://orcid.org/0000-0003-2866-6237>

André Anders  <https://orcid.org/0000-0002-5313-6505>

Robert Franz  <https://orcid.org/0000-0003-4842-7276>

References

- [1] Pfeiler M, Fontalvo G, Wagner J, Kutschej K, Penoy M, Michotte C, Mitterer C and Kathrein M 2008 Arc evaporation of Ti–Al–Ta–N coatings: the effect of bias voltage and Ta on high-temperature tribological properties *Tribol. Lett.* **30** 91–7
- [2] Grossmann B, Tkadletz M, Schalk N, Czettel C, Pohler M and Mitterer C 2018 High-temperature tribology and oxidation of $\text{Ti}(1-x-y)\text{Al}(x)\text{Ta}(y)_n$ hard coatings *Surf. Coat. Technol.* **342** 190–7
- [3] Trittemmel C, Daniel R, Lechthaler M, Rudigier H, Polcik P and Mitterer C 2012 Microstructure and mechanical properties of nanocrystalline Al–Cr–B–N thin films *Surf. Coat. Technol.* **213** 1–7
- [4] Rovere F, Music D, Schneider J and Mayrhofer P 2010 Experimental and computational study on the effect of yttrium on the phase stability of sputtered Cr–Al–Y–N hard coatings *Acta Mater.* **58** 2708–15
- [5] Anders A 2009 *Cathodic Arcs: From Fractal Spots to Energetic Condensation* (New York: Springer)
- [6] Sasaki J, Sugiyama K, Yao X and Brown I G 1993 Multiple-species ion beams from titanium-hafnium alloy cathodes in vacuum arc plasmas *J. Appl. Phys.* **73** 7184–7
- [7] Eriksson A, Zhirkov I, Dahlgvist M, Jensen J, Hultman L and Rosen J 2013 Characterization of plasma chemistry and ion energy in cathodic arc plasma from Ti–Si cathodes of different compositions *J. Appl. Phys.* **113** 163304
- [8] Zhirkov I, Eriksson A O and Rosén J 2013 Ion velocities in direct current arc plasma generated from compound cathodes *J. Appl. Phys.* **114** 213302
- [9] Nikolaev A G, Oks E M, Savkin K P, Yushkov G Y, Frolova V P and Barengolts S A 2014 Charge state, angular distribution, and kinetic energy of ions from multicomponent-cathodes in vacuum arc devices *J. Appl. Phys.* **116** 213303
- [10] Zhirkov I, Eriksson A, Petruhins A, Dahlgvist M, Ingason A S and Rosén J 2014 Effect of Ti–Al cathode composition on plasma generation and plasma transport in direct current vacuum arc *J. Appl. Phys.* **115** 123301
- [11] Anders A, Yotsombat B and Binder R 2001 Correlation between cathode properties, burning voltage, and plasma parameters of vacuum arcs *J. Appl. Phys.* **89** 7764–71
- [12] Anders A, Oks E M and Yushkov G Y 2005 Cathodic arcs: fractal voltage and cohesive energy rule *J. Appl. Phys.* **86** 211503
- [13] Yushkov G Y, Anders A, Oks E M and Brown I G 2000 Ion velocities in vacuum arc plasmas *J. Appl. Phys.* **88** 5618–22
- [14] Rosén J, Schneider J M and Anders A 2006 Charge state dependence of cathodic vacuum arc ion energy and velocity distributions *J. Appl. Phys.* **89** 141502
- [15] Rosén J, Anders A, Mráz S, Atiser A and Schneider J M 2006 Influence of argon and oxygen on charge-state-resolved ion energy distributions of filtered aluminum arcs *J. Appl. Phys.* **99** 123303
- [16] Franz R, Polcik P and Anders A 2013 Ion charge state distributions of Al and Cr in cathodic arc plasmas from composite cathodes in vacuum, argon, nitrogen, and oxygen *IEEE Trans. Plasma Sci.* **41** 1929–37
- [17] Eriksson A O, Mráz S, Jensen J, Hultman L, Zhirkov I, Schneider J M and Rosen J 2014 Influence of Ar and N_2 pressure on plasma chemistry, ion energy, and thin film composition during filtered arc deposition from Ti_3SiC_2 cathodes *IEEE Trans. Plasma Sci.* **42** 3498–507
- [18] Franz R, Polcik P and Anders A 2015 Element- and charge-state-resolved ion energies in the cathodic arc plasma from composite AlCr cathodes in argon, nitrogen and oxygen atmospheres *Surf. Coat. Technol.* **272** 309–21
- [19] Zhirkov I, Oks E and Rosen J 2015 Effect of N_2 and Ar gas on DC arc plasma generation and film composition from Ti–Al compound cathodes *J. Appl. Phys.* **117** 213301
- [20] Anders A 1999 Plasma fluctuations, local partial saha equilibrium, and the broadening of vacuum-arc ion charge state distributions *IEEE Trans. Plasma Sci.* **27** 1060–7

- [21] Anders A 2012 The evolution of ion charge states in cathodic vacuum arc plasmas: a review *Plasma Sources Sci. Technol.* **21** 035014
- [22] Anders A, Oks E M and Yushkov G Y 2007 Production of neutrals and their effects on the ion charge states in cathodic vacuum arc plasmas *J. Appl. Phys.* **102** 043303
- [23] Zöhrer S, Anders A and Franz R 2018 Time-resolved ion energy and charge state distributions in pulsed cathodic arc plasmas of NbAl cathodes in high vacuum *Plasma Sources Sci. Technol.* **27** 055007
- [24] MacGill R A, Dickinson M R, Anders A, Monteiro O R and Brown I G 1998 Streaming metal plasma generation by vacuum arc plasma guns *Rev. Sci. Instrum.* **69** 801–3
- [25] Lide D R 2008 *CRC Handbook of Chemistry and Physics* 89th edn (Boca Raton, FL: CRC Press) p 203
- [26] Tanaka K, Han L, Zhou X and Anders A 2015 Adding high time resolution to charge-state-specific ion energy measurements for pulsed copper vacuum arc plasmas *Plasma Sources Sci. Technol.* **24** 045010
- [27] Anders A 2005 The fractal nature of vacuum arc cathode spots *IEEE Trans. Plasma Sci.* **33** 1456–64
- [28] Rosen J and Anders A 2005 Time and material dependence of the voltage noise generated by cathodic vacuum arcs *J. Phys. D: Appl. Phys.* **38** 4184
- [29] Agarwal M S and Holmes R 1984 Arcing voltage of the metal vapour vacuum arc *J. Phys. D: Appl. Phys.* **17** 757
- [30] Anders A 2001 A periodic table of ion charge-state distributions observed in the transition region between vacuum sparks and vacuum arcs *IEEE Trans. Plasma Sci.* **29** 393–8
- [31] Galvin J E, Brown I G and MacGill R A 1990 Charge state distribution studies of the metal vapor vacuum arc ion source *Rev. Sci. Instrum.* **61** 583–5
- [32] Nikolaev A G, Yushkov G Y, Savkin K P and Oks E M 2012 Angular distribution of plasma in the vacuum arc ion source *Rev. Sci. Instrum.* **83** 02A503
- [33] Nikolaev A G, Savkin K P, Yushkov G Y and Oks E M 2014 Ion angular distribution in plasma of vacuum arc ion source with composite cathode and elevated gas pressure *Rev. Sci. Instrum.* **85** 02B501
- [34] Anders A 2005 Time-dependence of ion charge state distributions of vacuum arcs: an interpretation involving atoms and charge exchange collisions *IEEE Trans. Plasma Sci.* **33** 205–9
- [35] Anders A 1997 Ion charge state distributions of vacuum arc plasmas: the origin of species *Phys. Rev. E* **55** 969
- [36] Zhirkov I, Oks E and Rosen J 2015 Experimentally established correlation between ion charge state distributions and kinetic ion energy distributions in a direct current vacuum arc discharge *J. Appl. Phys.* **117** 093301
- [37] Mesyats G A 2013 Ecton mechanism of the cathode spot phenomena in a vacuum arc *IEEE Trans. Plasma Sci.* **41** 676–94
- [38] Krasov V I and Paperny V L 2017 Expansion of a multicomponent current-carrying plasma jet into vacuum *Plasma Phys. Rep.* **43** 298–306